01

Simulation of the three-qubit repetition code on the chain of superconducting qubits with couplers

© N.G. Berezkin[1–3], I.A. Simakov[1,2], G.S. Mazhorin[1,2]

[1] National University of Science and Technology MISIS, Moscow, Russia
[2] Russian Quantum Center, Moscow, Russia
[3] Moscow Institute of Physics and Technology (National Research University), Dolgoprudny, Moscow Region, Russia
E-mail: berezkin.ng@phystech.edu

Received July 22, 2025
Revised August 18, 2025
Accepted August 25, 2025

In superconducting quantum circuits, a promising method for implementing high-fidelity two-qubit gates is the microwave drive of a coupler. This paper presents the simulation of the three-qubit repetition code, taking into account the physical mechanism of two-qubit operation implementation: the effect of parasitic population of the excited state of the coupler is investigated, and the successful correction of this error using quantum error correction codes is demonstrated.

Keywords: superconducting qubits, coupler, microwave gates, repetition code, leakages from computational subspace.

DOI: 10.61011/TPL.2025.11.62220.20451

Quantum error-correcting codes are needed to implement fault-tolerant scalable quantum computing. Error detection with superconducting qubits has been demonstrated for the first time in pioneering study [1]. Tabilizing error-correcting codes, such as a repetition code [2] and a surface code [3], are currently the ones that were studied in most detail. Sequential error detection with a repetition code has been demonstrated for the first time in [4] in experiments with superconducting qubits, and a surface code was implemented in [5]. Surface code scaling was accomplished in pioneering studies [6,7] with superconducting processors, and a logical qubit surpassing in coherence characteristics all the physical qubits on which it is encoded was demonstrated. Other experimentally implemented quantum error correction algorithms (e.g., LDPC codes [8,9]) are also known. Alongside with superconducting qubits, other platforms for fault-tolerant quantum computing (ions [10] and neutral atoms [11]) are being developed.

In stabilizing error correction codes, logical quantum states are protected from noise by encoding them using a set of physical qubits that are called data qubits. The measurement of ancillary qubits positioned between the data ones provides an opportunity to determine the parity of state of adjacent data qubits, a change in which is indicative of an error. Arbitrary perturbations of states of data qubits are transformed into a composition of discrete X and Z errors due to projective measurements of ancillary qubits, the results of which are referred to as error syndromes [2,3,12]. In order to determine what the errors were and which qubits were affected, sequences of measured error syndromes are decoded using classical algorithms. One problem with this approach is that leakages from the computational subspace are not transformed into X or Z errors in measurements of ancillary qubits [13]. Leaks are characteristic of superconducting qubits, which are multi-level systems with a computational subspace of two lowest energy states. Moreover, non-computational states of superconducting qubits may be used to implement multi-qubit gates [14–16], where imperfect calibration translates into residual populations of non-computational levels.

A promising (in terms of scalability) option for implementing tunable coupling between superconducting qubits is the use of a coupler qubit (C) between computational qubits (Q). One way to perform two-qubit operations in such an architecture is microwave excitation of the coupler. This microwave scheme is implemented with fluxonium qubits serving as computational ones and transmons or fluxoniums used as couplers [15,16]. Among the advantages of microwave operations in the QCQ architecture are the suppression of ZZ interactions between computational qubits to a level of several kilohertz and the non-necessity of detuning of the magnetic flux from the optimal value at which the maximum qubit coherence times are achieved [17]. This helps achieve high entanglement efficiency combined with low parasitic interactions in the idle state.

The operation of microwave gates relies on the strong interaction between a coupler and computational qubits. It induces a dispersion shift (on the order of 100 MHz) [15,16] of the first excited state of a coupler qubit, which depends on the states of two adjacent computational qubits (Fig. 1, *a*). Therefore, the frequency detuning of the control signal from the transition frequency of the coupler qubit depends on the states of computational qubits, which translates into different phases at computational states.

A method for implementing a CZ gate in the Q_1CQ_2 architecture through the application of a 2π pulse with

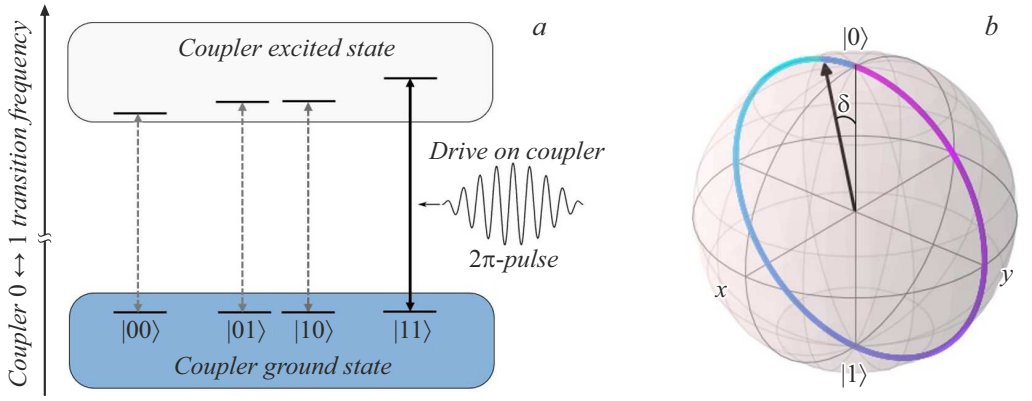

Figure 1. Experimental implementation of a CZ gate. a — 0–1 transition of the coupler that depends on the states of neighboring computational qubits. b — Trajectory of the state vector of the coupler qubit and its final position on the Bloch sphere after the CZ operation. The deviation by angle δ from state $|0\rangle$ is caused by the 2π-pulse calibration error.

a frequency close to the $|101\rangle_{Q_1CQ_2}$–$|111\rangle_{Q_1CQ_2}$ transition to the coupler was proposed in [15]. Conditional phase π is accumulated in computational state $|11\rangle_{Q_1Q_2}$ over the period of Rabi oscillations. Setting the microwave frequency close to the $|101\rangle_{Q_1CQ_2}$–$|111\rangle_{Q_1CQ_2}$ transition, one may excite oscillations between these states only, leaving the others unaffected. To achieve high two-qubit gate fidelity, the coupler must return to the ground state at the end of the pulse. In practice, a certain small population may remain in the excited state of the coupler qubit, which is attributable primarily to imperfect calibration of the 2π pulse (Fig. 1, b). This leakage from the computational subspace calls into question the possibility of application of microwave operations in standard correction algorithms. Specifically, the mentioned parasitic population interferes with single-qubit operations, altering the frequency of adjacent computational qubits. To test the performance of the correction code in this architecture, one needs to simulate it with account for the population of the coupler.

The possibility of correcting the leakage into the excited state of the coupler with stabilizing codes was investigated using the example of a three-qubit repetition code (Fig. 2, a). The logical state is encoded in the three-qubit repetition code by three data qubits, and error syndromes are measured with the use of two ancillary qubits by performing successive CNOT operations and measuring the states of the ancillary qubits. If p is the probability of occurrence of an independent physical error within one correction cycle, then the probability of a logical error after the execution of the correction algorithm at small p is proportional, in the leading order, to p^2, which is what is behind the advantage that the three-qubit repetition code provides [2].

In experiments, a CNOT gate is implemented by performing the CZ operation between data qubit D and ancillary qubit A, which is preceded and followed by Hadamard operators H on the ancillary qubit. We present the CZ operation as X-rotation by angle $\varphi = 2\pi + \delta$ between states $|101\rangle_{DCA}$ and $|111\rangle_{DCA}$, where $\delta \ll 1$ is the systematic calibration error. The corresponding unitary operator in the data–coupler–ancillary qubits basis $|DCA\rangle$ is

$$U_{\mathrm{CZ}} = \begin{pmatrix} 1 & 0 & 0 & 0 & 0 & 0 & 0 & 0 \\ 0 & 1 & 0 & 0 & 0 & 0 & 0 & 0 \\ 0 & 0 & 1 & 0 & 0 & 0 & 0 & 0 \\ 0 & 0 & 0 & 1 & 0 & 0 & 0 & 0 \\ 0 & 0 & 0 & 0 & 1 & 0 & 0 & 0 \\ 0 & 0 & 0 & 0 & 0 & \cos\frac{\varphi}{2} & 0 & -i\sin\frac{\varphi}{2} \\ 0 & 0 & 0 & 0 & 0 & 0 & 1 & 0 \\ 0 & 0 & 0 & 0 & 0 & -i\sin\frac{\varphi}{2} & 0 & \cos\frac{\varphi}{2} \end{pmatrix}. \quad (1)$$

In addition, we assume that the Hadamard operator fails if at least one of the adjacent couplers is in an excited state. This corresponds to an inverted control input at the coupler qubit in the circuit. The corresponding unitary operator in the coupler–ancillary–coupler qubits basis $|CAC\rangle$ is

$$U_H = \begin{pmatrix} \frac{1}{\sqrt{2}} & 0 & \frac{1}{\sqrt{2}} & 0 & 0 & 0 & 0 & 0 \\ 0 & 1 & 0 & 0 & 0 & 0 & 0 & 0 \\ \frac{1}{\sqrt{2}} & 0 & -\frac{1}{\sqrt{2}} & 0 & 0 & 0 & 0 & 0 \\ 0 & 0 & 0 & 1 & 0 & 0 & 0 & 0 \\ 0 & 0 & 0 & 0 & 1 & 0 & 0 & 0 \\ 0 & 0 & 0 & 0 & 0 & 1 & 0 & 0 \\ 0 & 0 & 0 & 0 & 0 & 0 & 1 & 0 \\ 0 & 0 & 0 & 0 & 0 & 0 & 0 & 1 \end{pmatrix}. \quad (2)$$

If data qubits are prepared in logical state $|0\rangle_L = |000\rangle_{D_1D_2D_3}$, calibration error δ does not lead to errors, since the sequential application of operators U_H, U_{CZ}, and U_H preserves all qubits in the ground state. However, error δ will have consequences for logical state $|1\rangle_L = |111\rangle_{D_1D_2D_3}$. Let us consider an example scenario of emergence of errors in application of the repetition code to logical state $|1\rangle_L$ (Fig. 2, b). It is assumed that an error syndrome measurement is performed at data qubits D_1 and D_2 with the use of ancillary qubit A_1, which is connected to the data qubits via couplers C_1 and C_2. In this example, the quantum circuit is assumed to have no other error channels (unrelated to the population of the coupler). Subjecting state $|D_1C_1A_1C_2D_2\rangle^{(0)} = |10001\rangle$ to

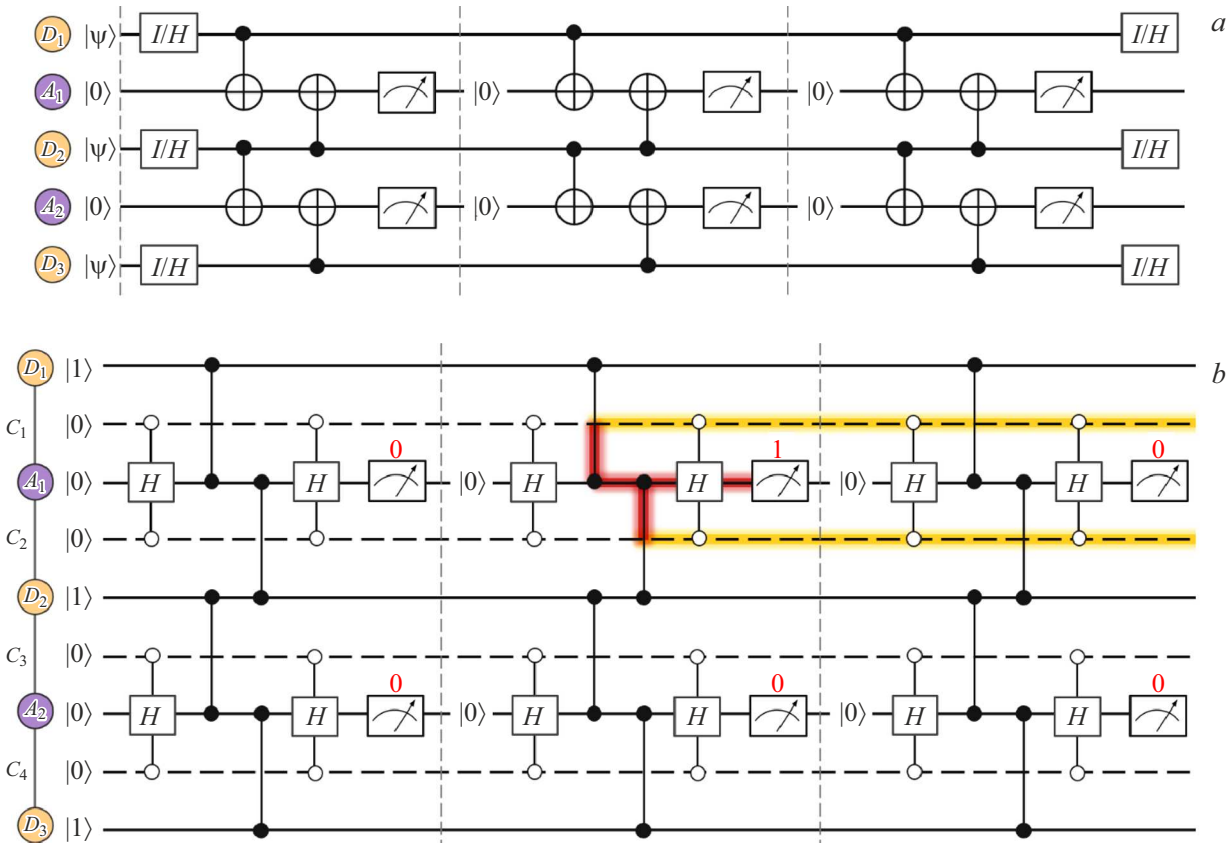

Figure 2. *a* — Three-qubit repetition code correcting X or Z errors (three correction cycles are shown). *b* — Example of propagation of an error at a coupler in the three-qubit repetition code correcting X errors. Scenario $|0\rangle_{A_1} \to |1\rangle_{A_1} \to |0\rangle_{A_1}$ is illustrated. The quantum circuit encodes logical state $|1\rangle_L$. D_1, D_2, and D_3 — data qubits; A_1 and A_2 — ancillary qubits; C_1, C_2, C_3, and C_4 — couplers.

quantum operations from the correction cycle, one obtains the following entangled state:

$$|D_1C_1A_1C_2D_2\rangle^{(1)} = \frac{1}{2}\left(1+\cos^2\frac{\delta}{2}\right)|10001\rangle + \frac{1}{2}\left(1-\cos^2\frac{\delta}{2}\right)|10101\rangle - \frac{\sqrt{2i}}{4}\sin\delta\left(|10111\rangle + |11101\rangle\right) - \frac{1}{\sqrt{2}}\sin^2\frac{\delta}{2}|11111\rangle. \quad (3)$$

According to expression (3), when the state of ancillary qubit A_1 is measured, state $|0\rangle_{A_1}$ will be obtained with a probability of

$$|(1+\cos^2(\delta/2))/2|^2 = 1-\delta^2/4+O(\delta^3).$$

The probability to obtain state $|1\rangle_{A_1}$, which is an incorrect result of measuring the parity of state of data qubits D_1 and D_2, is $\delta^2/4+O(\delta^3)$. The repetition of this error in several cycles in a row may lead to incorrect decoding of the measured syndromes and, consequently, logical errors.

Table 1. Asymptotic probabilities of error scenarios associated with the coupler population in three correction cycles

Number of errors	Scenario	Probability
0	$\|0\rangle \to \|0\rangle \to \|0\rangle$	$1-\frac{3}{4}p_c+O(p_c^{3/2})$
1	$\|1\rangle \to \|0\rangle \to \|0\rangle$ $\|0\rangle \to \|1\rangle \to \|0\rangle$ $\|0\rangle \to \|0\rangle \to \|1\rangle$	$\frac{1}{4}p_c+O(p_c^2)$
2	$\|1\rangle \to \|1\rangle \to \|0\rangle$ $\|0\rangle \to \|1\rangle \to \|1\rangle$ $\|1\rangle \to \|0\rangle \to \|1\rangle$	$\frac{1}{256}p_c^3+O(p_c^4)$
3	$\|1\rangle \to \|1\rangle \to \|1\rangle$	$\frac{1}{1024}p_c^5+O(p_c^6)$

Let us introduce quantity $p_c = \delta^2$: parameter of the physical error associated with the coupler population. Calculating states $|D_1C_1A_1C_2D_2\rangle^{(i)}$ after the ith correction cycle, one may find the asymptotic values of probabilities of various scenarios of measurement of error syndromes $|x_1\rangle_{A_1} \to |x_2\rangle_{A_1} \to \cdots \to |x_N\rangle_{A_1}$, where $|x_i\rangle_{A_1}$ is the result of measuring ancillary qubit A_1 within the i-th correction cycle. For example, if we consider a chain of three

Table 2. Error model used to simulate the three-qubit repetition code

Physical error	Parameter
Relaxation	$\gamma_1 = \frac{\tau}{T_1}$ — ratio of operation time τ and relaxation time T_1
Pure dephasing	$\gamma_\phi = \frac{\tau}{T_\phi}$ — ratio of operation time τ and pure dephasing time T_ϕ
Readout error	p_m — probability of an X error in measurement of an ancillary qubit
Leakage to the excited state of a coupler qubit	$p_c = \delta^2$, δ — systematic error of calibration of a 2π pulse

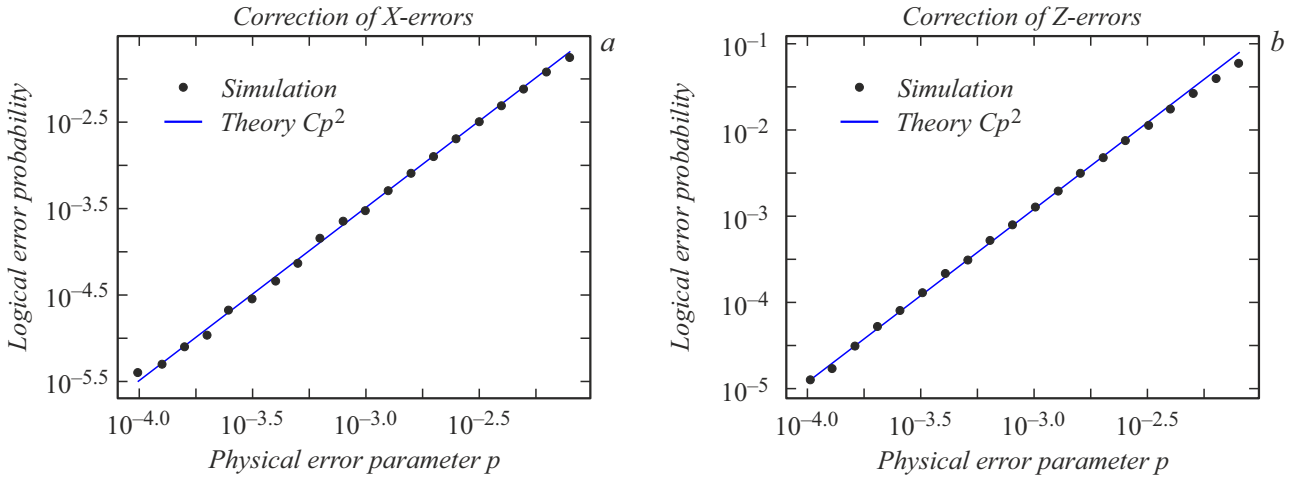

Figure 3. Dependences of the logical error probability on physical error parameter p for the repetition code correcting X errors (a) and Z errors (b). Dots and lines represent the results of simulation and the theoretical quadratic dependence, respectively.

correction cycles, the probability of favorable scenario $|0\rangle_{A_1} \to |0\rangle_{A_1} \to |0\rangle_{A_1}$ is $1 - 3p_c/4 + O(p_c^{3/2})$. The probabilities of scenarios with one error in three correction cycles are $p_c/4 + O(p_c^2)$. These probabilities are linear with respect to parameter p_c, but such scenarios will not lead to logical errors: the decoder will process them correctly in the same way as ancillary qubit readout errors. The asymptotic probabilities of other scenarios are listed in Table 1. Calculations revealed that the probabilities of scenarios with two errors in three cycles are, in the leading order, proportional to p_c^3, which exceeds the correction limit of the three-qubit repetition code. Thus, the imperfection of a CNOT gate does not in itself lead to logical errors with their probability linear in parameter p_c. This gives reason to believe that the repetition code will work efficiently in the proposed error model where the coupler influence is taken into account.

Simulation was performed in order to test the performance of the correction code in the considered architecture. The error model used in calculations included relaxation and pure dephasing channels [18], the ancillary qubit readout error, and the influence of coupler qubits discussed above. The parameters characterizing each physical error are presented in Table 2. In calculations, all these parameters were assumed to be equal to p (physical error parameter). The performance criterion of the three-qubit repetition code is a parabolic dependence of the probability of a logical error on the introduced physical error parameter p. The Qiskit library [19] was used to simulate quantum circuits. The MWPM (minimum weight-perfect matching) algorithm was used to decode error syndromes [20]. The repetition code correcting X and Z- errors was simulated separately. In the repetition codes correcting X- and Z errors, data qubits were initialized in states $|0\rangle_L$, $|1\rangle_L$ and $|+\rangle_L$, $|-\rangle_L$, respectively. Twenty correction cycles were performed in each algorithm. To gather statistics, both algorithms were run $2 \cdot 10^6$ times. Quadratic dependences of the probability of a logical error on the physical error parameter were obtained in each simulation experiment (Fig. 3). Thus, it was demonstrated that the error associated with the population of couplers is corrected successfully by the repetition code.

Acknowledgments

The authors wish to thank A.V. Ustinov for valuable comments and helpful remarks that contributed to improving the manuscript.

Funding

This study was supported financially by the Ministry of Science and Higher Education of the Russian Federation as part of the „Priority 2030" academic leadership program (strategic project „Quantum Internet").

Conflict of interest

The authors declare that they have no conflict of interest.

References

[1] A.D. Córcoles, E. Magesan, S.J. Srinivasan, A.W Cross, M. Steffen, J.M. Gambetta, J.M. Chow, Nat. Commun., **6**, 6979 (2015). DOI: 10.1038/ncomms7979
[2] S.J. Devitt, W.J. Munro, K. Nemoto, Rep. Prog. Phys., **76** (7), 076001 (2013). DOI: 10.1088/0034-4885/76/7/076001
[3] A.G. Fowler, M. Mariantoni, J.M. Martinis, A.N. Cleland, Phys. Rev. A, **86** (3), 032324 (2012). DOI: 10.1103/PhysRevA.86.032324
[4] J. Kelly, R. Barends, A.G. Fowler, A. Megrant, E. Jeffrey, T.C. White, D. Sank, J.Y. Mutus, B. Campbell, Y. Chen, Z. Chen, B. Chiaro, A. Dunsworth, I.-C. Hoi, C. Neill, P.J.J. O'Malley, C. Quintana, P. Roushan, A. Vainsencher, J. Wenner, A.N. Cleland, J.M. Martinis, Nature, **519**, 66 (2015). DOI: 10.1038/nature14270
[5] C.K. Andersen, A. Remm, S. Lazar, S. Krinner, N. Lacroix, G.J. Norris, M. Gabureac, C. Eichler, A. Wallraff, Nat. Phys., **16**, 875 (2020). DOI: 10.1038/s41567-020-0920-y
[6] Google Quantum AI and Collaborators, Nature, **614**, 676 (2023). DOI: doi.org/10.1038/s41586-022-05434-1
[7] Google Quantum AI and Collaborators, Nature, **638**, 920 (2025). DOI: 10.1038/s41586-024-08449-y
[8] N.P. Breuckmann, J.N. Eberhardt, PRX Quantum, **2**, 040101 (2021). DOI: 10.1103/PRXQuantum.2.040101
[9] K. Wang, Z. Lu, C. Zhang, G. Liu, J. Chen, Y. Wang, Y. Wu, S. Xu, X. Zhu, F. Jin, Y. Gao, Z. Tan, Z. Cui, N. Wang, Y. Zou, A. Zhang, T. Li, F. Shen, J. Zhong, Z. Bao, Z. Zhu, Y. Han, Y. He, J. Shen, H. Wang, J.-N. Yang, Z. Song, J. Deng, H. Dong, Z.-Z. Sun, W. Li, Q. Ye, S. Jiang, Y. Ma, P.-X. Shen, P. Zhang, H. Li, Q. Guo, Z. Wang, C. Song, H. Wang, D.-L. Deng, arXiv:2505.09684 [quant-ph] (2025). DOI: 10.48550/arXiv.2505.09684
[10] B.W. Reichardt, D. Aasen, R. Chao, A. Chernoguzov, W. van Dam, J.P. Gaebler, D. Gresh, D. Lucchetti, M. Mills, S.A. Moses, B. Neyenhuis, A. Paetznick, A. Paz, P.E. Siegfried, M.P. da Silva, K.M. Svore, Z. Wang, M. Zanner, arXiv:2409.04628 [quant-ph] (2024). DOI: 10.48550/arXiv.2409.04628
[11] B.W. Reichardt, A. Paetznick, D. Aasen, I. Basov, J.M. Bello-Rivas, P. Bonderson, R. Chao, W. van Dam, M.B. Hastings, R.V. Mishmash, A. Paz, M.P. da Silva, A. Sundaram, K.M. Svore, A. Vaschillo, Z. Wang, M. Zanner, W.B. Cairncross, C.-A. Chen, D. Crow, H. Kim, J.M. Kindem, J. King, M. McDonald, M.A. Norcia, A. Ryou, M. Stone, L. Wadleigh, K. Barnes, P. Battaglino, T.C. Bohdanowicz, G. Booth, A. Brown, M.O. Brown, K. Cassella, R. Coxe, J.M. Epstein, M. Feldkamp, C. Griger, E. Halperin, A. Heinz, F. Hummel, M. Jaffe, A.M.W. Jones, E. Kapit, K. Kotru, J. Lauigan, M. Li, J. Marjanovic, E. Megidish, M. Meredith, R. Morshead, J.A. Muniz, S. Narayanaswami, C. Nishiguchi, T. Paule, K.A. Pawlak, K.L. Pudenz, D. Rodríguez Pérez, J. Simon, A. Smull, D. Stack, M. Urbanek, R.J.M. van de Veerdonk, Z. Vendeiro, R.T. Weverka, T. Wilkason, T.-Y. Wu, X. Xie, E. Zalys-Geller, X. Zhang, B.J. Bloom, arXiv:2411.11822 [quant-ph] (2024). DOI: 10.48550/arXiv.2411.11822
[12] Z. Chen, K. Satzinger, J. Atalaya, A. Dunsworth, D. Sank, C. Quintana, M. McEwen, R. Barends, P. Klimov, S. Hong, C. Jones, A. Petukhov, D. Kafri, S. Demura, B. Burkett, C. Gidney, A. Fowler, A. Paler, J. Kelly, Nature, **595**, 383 (2021). DOI: 10.1038/s41586-021-03588-y
[13] B. Varbanov, F. Battistel, B. Tarasinski, V. Ostroukh, T. O'Brien, L. DiCarlo, B. Terhal, npj Quantum Inf., **6**, 102 (2020). DOI: 10.1038/s41534-020-00330-w
[14] Q. Ficheux, L.B. Nguyen, A. Somoroff, H. Xiong, K.N. Nesterov, M.G. Vavilov, V.E. Manucharyan, Phys. Rev. X, **11**, 021026 (2021). DOI: 10.1103/PhysRevX.11.021026
[15] I.A. Simakov, G.S. Mazhorin, I.N. Moskalenko, N.N. Abramov, A.A. Grigorev, D.O. Moskalev, A.A. Pishchimova, N.S. Smirnov, E.V. Zikiy, I.A. Rodionov, I.S. Besedin, PRX Quantum, **4**, 040321 (2023). DOI: 10.1103/PRXQuantum.4.040321
[16] L. Ding, M. Hays, Y. Sung, B. Kannan, J. An, A. Di Paolo, A.H. Karamlou, T.M. Hazard, K. Azar, D.K. Kim, B.M. Niedzielski, A. Melville, M.E. Schwartz, J.L. Yoder, T.P. Orlando, S. Gustavsson, J.A. Grover, K. Serniak, W.D. Oliver, Phys. Rev. X, **13**, 031035 (2023). DOI: 10.1103/PhysRevX.13.031035
[17] I.N. Moskalenko, I.A. Simakov, N.N. Abramov, A.A. Grigorev, D.O. Moskalev, A.A. Pishchimova, N.S. Smirnov, E.V. Zikiy, I.A. Rodionov, I.S. Besedin, npj Quantum Inf., **8**, 130 (2022). DOI: 10.1038/s41534-022-00644-x
[18] M. Nielsen, I. Chuang, *Kvantovye vychisleniya i kvantovaya informatsiya* (Mir, M., 2006), pp. 471–480 (in Russian).
[19] A. Javadi-Abhari, M. Treinish, K. Krsulich, C.J. Wood, J. Lishman, J. Gacon, S. Martiel, P.D. Nation, L.S. Bishop, A.W. Cross, B.R. Johnson, J.M. Gambetta, arXiv:2405.08810 [quant-ph] (2024). DOI: 10.48550/arXiv.2405.08810
[20] S.T. Spitz, B. Tarasinski, C.W.J. Beenakker, T.E. O'Brien, Adv. Quantum Technol., **1** (1), 1800012 (2018). DOI: 10.1002/qute.201870015

Translated by D.Safin